



Super-telomeres in transformed human fibroblasts

Ilaria Chiodi^a, Cristina Belgiovine^a, Samantha Zongaro^{a,1}, Roberta Ricotti^a, Beatrice Horard^{b,2}, Andrea Lossani^a, Federico Focher^a, Eric Gilson^{b,c,d}, Elena Giulotto^e, Chiara Mondello^{a,*}

^a Istituto di Genetica Molecolare, CNR, via Abbiategrosso 207, 27100 Pavia, Italy

^b Laboratoire de Biologie Moléculaire de la Cellule, CNRS UMR5239, Ecole Normale Supérieure de Lyon, UCBL1, IFR128, 46 allée d'Italie, 69364 Lyon Cedex 07, France

^c Institute for Research on Cancer and Aging, Nice (IRCAN), CNRS UMR7284/INSERM U1081, Faculty of Medicine, Nice, France

^d Department of Medical Genetics, Archet 2 Hospital, CHU of Nice, France

^e Dipartimento di Biologia e Biotecnologie "Lazzaro Spallanzani", Università di Pavia, via Ferrata 9, 27100 Pavia, Italy

ARTICLE INFO

Article history:

Received 3 January 2013

Received in revised form 22 March 2013

Accepted 29 March 2013

Available online 6 April 2013

Keywords:

Telomere

Telomerase

Telomeric protein

DNA methylation

Telomere positioning effect

ABSTRACT

Telomere length maintenance is critical for organisms' long-term survival and cancer cell proliferation. Telomeres are kept within species-specific length ranges by the interplay between telomerase activity and telomeric chromatin organization. In this paper, we exploited telomerase immortalized human fibroblasts (cen3tel) that gradually underwent neoplastic transformation during culture propagation to study telomere composition and length regulation during the transformation process. Just after telomerase catalytic subunit (hTERT) expression, cen3tel telomeres shortened despite the presence of telomerase activity. At a later stage and concomitantly with transformation, cells started elongating telomeres, which reached a mean length greater than 100 kb in about 900 population doublings. Super-telomeres were stable and compatible with cell growth and tumorigenesis. Telomere extension was associated with increasing levels of telomerase activity that were linked to the deregulation of endogenous telomerase RNA (hTERC) and exogenous telomerase reverse transcriptase (hTERT) expression. Notably, the increase in hTERC levels paralleled the increase in telomerase activity, suggesting that this subunit plays a role in regulating enzyme activity. Telomeres ranging in length between 10 and more than 100 kb were maintained in an extendible state although TRF1 and TRF2 binding increased with telomere length. Super-telomeres neither influenced subtelomeric region global methylation nor the expression of the subtelomeric gene *FRG1*, attesting the lack of a clear-cut relationship between telomere length, subtelomeric DNA methylation and expression in human cells. The cellular levels of the telomeric proteins hTERT, TRF1, TRF2 and Hsp90 rose with transformation and were independent of telomere length, pointing to a role of these proteins in tumorigenesis.

© 2013 Elsevier B.V. All rights reserved.

1. Introduction

Telomeres are specialized nucleo-protein structures that protect human chromosome ends from nucleolytic digestion and end-to-end fusions, thus being essential for chromosome stability [1]. Human telomeric DNA is composed of tandem repetitions of the TTAGGG hexanucleotide, it is double stranded, except at the 3' region,

where it forms a 100–250 nucleotide long single strand overhang [2]. Because the extension of the repetitions varies from chromosome to chromosome and from cell to cell, telomeric DNA length is heterogeneous both within cells and among chromosomes of a single cell, but it is generally maintained within a species-specific range [3]. In human embryonic cells, for example, the average telomere length is around 15 kb; in contrast, in mice, telomeres can extend over 50 kb. Thus, mechanisms exist that restrain telomere length within a definite extension range.

Telomeres are associated with several proteins, which play an essential role in telomere maintenance. A six subunit complex (TRF1, TRF2, RAP1, TIN2, TPP1, POT1), named shelterin [4], specifically binds to telomeres and controls telomere stability and length. TRF1 and TRF2 act as *in cis* negative regulators of telomere elongation [5–7]. Evidence has been reported that TRF1 controls telomerase-mediated telomere lengthening through its interaction with POT1, which binds the telomeric single strand overhang and transduces TRF1 signals to telomerase, the enzyme deputed to telomere elongation [8].

* Corresponding author at: IGM-CNR, Via Abbiategrosso, 207, 27100 Pavia, Italy. Tel.: +39 0382 546332.

E-mail addresses: chiodi@igm.cnr.it (I. Chiodi), Cristina.Belgiovine@humanitasresearch.it (C. Belgiovine), zongaro@ipmc.cnrs.fr (S. Zongaro), ricotti@igm.cnr.it (R. Ricotti), beatrice.horard@univ-lyon1.fr (B. Horard), lossani@igm.cnr.it (A. Lossani), focher@igm.cnr.it (F. Focher), Eric.Gilson@ens-lyon.fr (E. Gilson), elena.giulotto@univp.it (E. Giulotto), mondello@igm.cnr.it (C. Mondello).

¹ Present address: Institut de Pharmacologie Moléculaire et Cellulaire, 660 Route des Lucioles Sophia Antipolis, 06560 Valbonne, France.

² Present address: Centre de Génétique et de Physiologie Moléculaires et Cellulaires-UMR CNRS 5534/Université Lyon 1, Villeurbanne, France.

Telomerase allows cells to overcome the end replication problem, which is due to the unidirectional and primer-dependent DNA polymerase synthetic activity. Telomerase is a ribonuclear-protein complex that elongates the 3' telomeric ends through a reverse-transcription reaction, using the RNA moiety (TERC) as template and the catalytic subunit (TERT) as enzymatic activity [9]. In human cells, together with TERC and TERT, the regulatory protein dyskerin is required for the formation of a catalytically active telomerase [10] and other proteins participate in telomerase biogenesis and regulation. hTERT (human TERT) expression is tightly regulated during development and its expression correlates with the presence of telomerase activity; in contrast, hTERC (human TERC) is constitutively expressed, even when telomerase is absent. hTERT is expressed at very low levels in most adult somatic cells [11], while is present in stem cells, germ-line and embryonic cells. In somatic cells, the low telomerase activity is not sufficient to maintain telomeres, which shorten at each cell division. When their length falls below a threshold level, telomeres trigger cellular senescence [12]. Senescent cells remain metabolically active even for years, but are unable to divide, because short telomeres are recognized as DNA double strand breaks and activate the DNA damage response that arrest cells' proliferation [13]. Thus, telomere shortening has been considered as a "mitotic clock" [14].

In contrast to normal somatic cells, telomerase is active in the vast majority of tumors (about 85%), in agreement with the requirement of functional telomeres for an indefinite cellular proliferation [15]. The necessity of preserving functional telomeres in tumor cells is confirmed by the observation that tumor cells lacking telomerase activity maintain telomeres through a recombination based mechanism known as alternative lengthening of telomeres (ALT) [16]. Characteristics of cells adopting this mechanism are a high frequency of sister chromatid exchanges between telomeres, leading to telomeres highly heterogeneous in length, extrachromosomal telomeric DNA circles and PML (Promyelocytic Leukemia) nuclear bodies containing telomeric chromatin (ALT PML bodies) [17].

In several somatic cells, ectopic hTERT expression is sufficient to induce telomerase activity, allows overcoming cellular senescence and leads to cellular immortalization [18,19]. In different hTERT immortalized cell lines, telomeres can reach different extensions and telomerase activity levels, as well as hTERT and hTERC expression, play a role in the determination of their length [20,21]. Very long telomeres, longer than 50 kb, were found in different cell types in which both hTERT and hTERC were ectopically expressed; these high levels of telomere elongation correlated with high degrees of telomerase activity [22,23].

By ectopic hTERT expression, we have obtained a human fibroblast cell line (named cen3tel) that has become immortal and has undergone neoplastic transformation during *in vitro* propagation [24–27]. The acquisition of the neoplastic phenotype was a gradual phenomenon; in fact, initially cells maintained a phenotype similar to that of parental fibroblasts (represented in this work by cells around population doubling, PD, 30), then (around PD 100) became able to grow in the absence of solid support, a feature typical of the initial phases of transformation [25]. Subsequently (around PD 160), cen3tel cells acquired the capacity to induce tumors in about one month when injected subcutaneously into immunocompromised mice and, upon further propagation in culture, they increased their aggressiveness, forming tumors with shorter latencies (~8 days around PD 600 and ~2 days around PD 1000). Moreover, cells around PD 1000 were also able to induce lung metastases when injected into the tail vein of nude mice [24,27]. In cen3tel cells, anchorage independent growth was associated with downregulation of the *CDKN2A* locus, while neoplastic transformation with p53 inactivation and c-MYC overexpression [27].

We also found that, after the transformation process, cen3tel cells lost the ability to regulate telomere length at a steady state level and reached an average telomere extension greater than 100 kb. In this

work, we investigated the mechanisms leading to the loss of telomere length homeostasis.

2. Materials and method

2.1. Cells and cell culture

Cen3tel cells were obtained from primary cen3 fibroblasts, by infection with an hTERT-containing retrovirus [25]. MDA-MB-231 (breast cancer), U373 (glioblastoma), primary cen3 and cen3tel cells were grown in Dulbecco's modified Eagle's Medium (DMEM, Euroclone) supplemented with 10% fetal bovine serum (Lonza), 2 mM glutamine, and 1% non-essential amino acids (Euroclone), 0.1 mg/ml penicillin (Euroclone), 100 U/ml streptomycin (Euroclone) at 37 °C in an atmosphere containing 5% CO₂. Cen3tel cells were used at different PDs comprised between PD 30 and PD 1200. To establish clonal cen3tel populations, single cells at PD 262 were seeded at low density (50 cells/10 cm diameter dish) and clones derived from a single cell were isolated and propagated *in vitro*. PD numbering of the clones was restarted, counting all the divisions performed by the single cell that generated the clone.

2.2. Analysis of telomere length and telomerase activity

Telomere length was determined by analyzing the mean length of the terminal restriction fragments (TRFs) by Southern blotting. For the analysis of TRFs below 20 kb, DNA samples were processed and hybridized as described in Mondello et al. [25]. For the analysis of longer telomeres, DNA samples were prepared from 10⁶ cells embedded in 2% InCert Agarose (Cambrex) and sequentially digested with 20 U of *AfaI* first and *HinfI* then. DNA fragments were separated through a 1% agarose gel in 0.5× TBE, using the CHEF-DR®II Pulsed Field Electrophoresis System (Bio-Rad). Separation was performed at 14 °C either for 13 h at 6 V/cm at a switch time of 0.5–2 s or for 16 h at 6 V/cm at a switch time of 5–20 s. Southern blot was then carried out as in [25]. The signal intensity along each lane was quantified by the Image-Quant software and the data were used to determine the mean length of TRFs as described by Harley et al. [28].

Telomeres were visualized on mitotic chromosomes by performing fluorescence *in situ* hybridization (FISH) on metaphase spreads using a FITC-labeled (ccctaa)₃ peptide nucleic acid probe (PNA, PerSeptive Biosystems) following the procedure set up by Lansdorp et al. [29], with minor modifications. Cells were denatured *in situ* at 70 °C for 2 min in 70% formamide, 1% Blocking Reagent (Roche), 10 mM Tris-HCl pH 7.0, 2 µg/ml PNA, and then hybridized at room temperature for 2 h. Washes were performed at room temperature in 70% formamide in 10 mM Tris-HCl pH 7.2, and then in 150 mM NaCl, 50 mM Tris-HCl pH 7.5, 0.05% Tween 20. Chromosomes were counter-stained with 0.2 µg/ml DAPI (4',6-diamidino-2-phenylindole) in PBS for 10 min. Slides were analyzed using an optical microscope Olympus IX71 equipped with a 100× objective. Images were acquired with a digital camera Cool SNAPES (Photometrics) using the MetaMorph software. Figures were assembled using Adobe Photoshop and Adobe Illustrator.

Telomerase activity was analyzed using the TRAPEZE kit (Chemicon) according to the manufacturer's instructions. DNA fragments were separated on polyacrylamide gels, which were stained for 15 min with 1× SYBR Gold Nucleic Acid Gel Stain (Molecular Probes, Life Technologies) in 0.5× TBE.

2.3. RNA extraction, reverse transcription-PCR (RT-PCR) and real-time RT-PCR

Total RNA was extracted from actively dividing cells using the Trizol reagent (Life Technologies). For RT-PCR, cDNA was generated from 1 µg of RNA using the QuantiTec Reverse Transcription Kit (Qiagen), following the manufacturer's instructions. cDNA (2 µl

each) was PCR amplified using 2 U Taq DNA polymerase (Promega). To detect the expression of endogenous hTERT, the primer RA58 (5'-ggctgaagtgtcacag) and the primer hTERT3'UTR (5'-ggccgagagcagaccagcagcc) in the 3' untranslated region [19] were used; PCR was carried out for 40 cycles with an annealing temperature (Ta) of 64 °C. As primers within the hTERT cDNA, the primers LT5 (5'-cgggaagagtgtctggagcaa) and LT6 (5'-ggatgaagcggagtctgga) [20] were used; PCR was carried out for 25 cycles with a Ta of 56 °C. For *FRG1* expression analysis the following primers were used: 1F (5'-tctacagagcagtaggctgca) and 9R (5'-ataaggcagaacaaaatccc); the primers for GAPDH were: forward 5'-accacagtccatgcatcac and reverse 5'-tccaccacctgtgtctgta. Semi-quantitative PCR was carried out for a number of cycles in the range of reactions' exponential phase (28 cycles with a Ta of 58 °C for *FRG1* and for 25 cycles with a Ta of 60 °C, for *GAPDH*). PCR products were analyzed on a 1.5% agarose gel stained with 1× SYBR Gold (Life Technologies) in 1× TBE as in the TRAP assay (see above). The primers for *Rpl13a* were acquired by Qiagen; PCR was carried out for 25 cycles with a Ta of 60 °C.

For the real-time RT-PCR experiments, the PD of cen3tel cells is not specified because more than one RNA sample was prepared and used for cen3tel cells around PD 30, 100, 160, 600 and 1000. Gene expression was quantified by SYBR Green chemistry using the QuantiTect SYBR Green Kit (Qiagen). For TERC, the primers TERC forward (5'-tctaaccctaactgagaagg) and TERC reverse (5'-gtttgctctagaagaacg) [30] were used. For TRF1, TRF2 and GusB dedicated sets of commercial primers (Qiagen) were used. Reactions were run in triplicate for each experimental point and each experiment was repeated at least twice. Real-time PCR was done on the Light Cycler 480 (Roche), using 96-well reaction plates. Raw data were normalized using the results obtained with the *GusB* housekeeping gene.

2.4. Western blotting

Whole-cell lysates for Western blot analysis were prepared lysing the cells in coimmunoprecipitation buffer (10 mM Tris-HCl (pH 7.6), 0.5% NP40, 140 mM NaCl, 5 mM EDTA (pH 8.0), 1× protease inhibitor cocktail (Sigma-Aldrich) and 2 mM NaVO₄). For each sample, 50 µg of protein extract were loaded onto the gels. The following antibodies were used: anti-hTERT (95110, DIESSE); anti-Hsp90 (N-17, Santacruz); anti-TRF1 (ab [57-6], Abcam); anti-TRF2 (clone 4A794, Upstate); anti-γ-tubulin (clone GTU-88, Sigma). All primary antibodies were probed by a secondary horseradish peroxidase-conjugated antibody (Jackson Laboratories). Chemiluminescent assay was used for detection (Super Signal West Pico, Pierce or Western C, Bio-Rad). The intensity of the bands was quantified using Image-Quant, corrected for the intensity of the bands in the loading control and then normalized either relatively to primary cen3 fibroblasts or to cen3tel cells at the earliest passage.

2.5. Chromatin immunoprecipitation (ChIP)

For ChIPs, cells were fixed for 10 min at room temperature adding formaldehyde in culture medium at a final concentration of 0.75%. Then, cells were lysed in 140 mM NaCl, 50 mM HEPES-KOH pH 7.5, 1 mM EDTA pH 8.0, 1% Triton X-100, 0.1% SDS, 0.1% Sodium deoxycholate and 1× protease inhibitor cocktail (Roche) at a density of 1.3×10^7 /ml. Lysates were sonicated to obtain chromatin fragments of 0.5–1 kb. 20–25 µg of chromatin of each sample were diluted in a final volume of 2 ml in binding buffer (150 mM NaCl, 20 mM Tris-HCl pH 8.0, 2 mM EDTA pH 8.0, 1% Triton X-100, 1× protease inhibitor cocktail) and pre-cleared with 20 µl of Protein A/G PLUS-Agarose beads (Santa Cruz Biotechnology) overnight at 4 °C. Samples were centrifuged and supernatants were incubated for 5 h at 4 °C with 4 µg of anti-TRF1 (N19-R, Santa Cruz Biotechnology) or anti-TRF2 (clone 4A794, Upstate) antibody and then supplemented with 80 µl of blocked beads and incubated overnight at 4 °C. Immunoprecipitated pellets were washed four times with binding buffer containing 150 mM NaCl

in the first three washes and 500 mM NaCl in the final wash. Chromatin was eluted from the beads with 100 mM NaHCO₃, 1% SDS for 15 min at room temperature. After the addition of 0.5 mg/ml RNase A, crosslinks were reversed overnight at 65 °C. In parallel, for each sample, an amount of chromatin equal to that used for the ChIP assays was processed to remove crosslinks and give rise to the total DNA samples. After this step, DNA was purified with Qiaquick PCR Purification Kit (Qiagen) and eluted with 50 µl water. Eluates were denatured and slot blotted onto Nytran Nylon membranes (Schleicher & Schuell); 80% of each immunoprecipitated sample was loaded for the detection of telomeric sequences and 20% for Alu sequences; 1% and 20% of each total DNA sample were loaded in parallel.

Membrane hybridization was performed overnight at 44 °C with a 5' ³²P- or digoxigenin (Dig)-labeled TELO probe (5'-(ccctaa)₅) or a Dig-labeled probe for the consensus sequence of the ALU-J subfamily (5'-gtgatccgcccctcgccctccaaagt, ALU probe). Membranes hybridized with the ³²P-labeled probes were exposed overnight to PhosphorImager screens; membranes hybridized with the Dig-labeled probe were incubated with an anti-Dig-HRP conjugated antibody (Jackson ImmunoResearch) and the signal was revealed using SuperSignal West Femto (Pierce). Quantification of the percentage of precipitated DNA was done with the QuantityOne software (Bio-Rad). The percentage of telomeric DNA immunoprecipitated in each cen3tel sample was calculated relatively to the telomeric signal in the corresponding total DNA. Therefore, the calculated ChIP yield takes into account changes in telomere length. ChIP experiments were repeated four times with the anti-TRF1 antibody and twice with the anti-TRF2 one.

2.6. DNA methylation of subtelomeric loci

Methylated DNA immunoprecipitation was performed as previously described [31,32]. Genomic DNA was isolated from cen3tel cells using DNeasy Blood and Tissue kit (Qiagen). 4 µg of genomic DNA was fragmented by sonication to sizes ranging from 200 bp to 1000 bp. Methylated DNA fragments were immunoprecipitated with an anti-5m-cytosine rabbit polyclonal antibody (MegabaseResearch #CP51000) or with rabbit IgG as control. Isolated DNA was subject to real-time PCR analysis. Primers sets for proximal subtelomeric region from chromosome 2 TRB1 repeats were 5'-tggacctaataatccgaaa and 5'-gctggacaccactgtaagca. Primer sets for the D4Z4 megasatellite found at 4q, 10q and 18p subtelomeric regions were 5'-ctcagcgaggaagaataccg and 5'-accgggcttagacctagaag. GAPDH promoter region was used as negative control, and primer sets were 5'-cgtgccagtgtaaccag and 5'-cgccgtaaaaccgtagta.

3. Results

3.1. Telomere length dynamics during cen3tel cell lifespan

Infection of primary cen3 fibroblasts with a retrovirus carrying the hTERT cDNA restored telomerase activity and allowed cells to become immortal, giving rise to the cen3tel cell population. We studied telomere length dynamics during culture propagation of the immortalized cells, between PD 30 and PD 1200, by analyzing the distribution of the terminal restriction fragments (TRFs) by Southern blotting with a probe for the telomeric repeats. Initially, DNA samples prepared from cells between PD 30 and PD 400 were analyzed after restriction enzyme digestion and separation by conventional gel electrophoresis (Fig. 1a). At these stages, we observed a peculiar telomere dynamics since telomeres kept on shortening up to about PD 100, the lowest mean TRF length, 5.7 kb, was found in cells at PD 112 (Fig. 1a lane 4), and then started to be elongated (see also [25]). Because in cells at the most advanced PDs, TRFs became too long to be resolved by conventional agarose gel electrophoresis, telomeric fragments obtained from cells from PD 167 up to PD 1200 were separated by

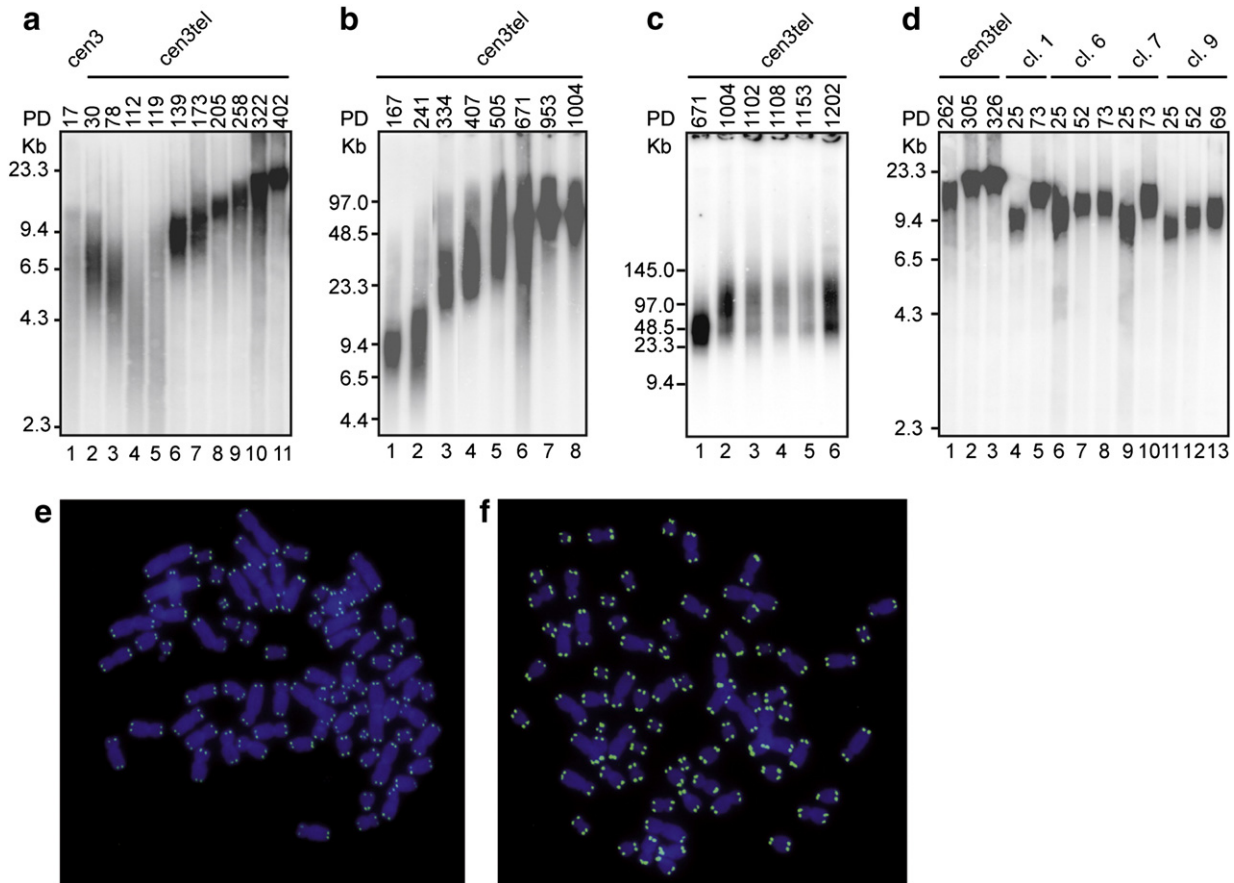


Fig. 1. Telomere length in cen3tel cells and clonal populations at different propagation stages. (a–d) Southern blot analysis of TRF distribution using a telomeric radioactive probe. Restriction enzyme digested DNA samples prepared from cen3 primary fibroblasts (a, lane 1), cen3tel cells at different PDs (a–c) or cen3tel clonal populations (d) were either separated on an agarose gel through conventional electrophoresis (a, d) or through pulse field gel electrophoresis (b) for 13 h at 6 V/cm at a switch time of 0.5–2 s or (c) for 16 h at 6 V/cm at a switch time of 5–20 s. Clonal populations were derived from cen3tel cells at PD 262 and were analyzed at different PDs together with their parental cells both at the stage at which they were seeded for clone isolation (panel d, lane 1) and at a later stage (panel d, lanes 2 and 3). PD numbering of the clones was restarted from the seeding of the cells (see [Materials and methods](#)). The size (kb) and the position of the molecular weight markers are indicated on the left. (e–f) FISH analysis of telomeres in cen3tel cells at PD 338 (e) and 775 (f) using a fluoresceine-labeled telomeric PNA probe (bright spots). Metaphases were counterstained with DAPI. Image acquisition was performed with the same exposure time to allow comparison of the hybridization signal intensity.

pulse field gel electrophoresis. To avoid DNA degradation, cell lysis and DNA restriction enzyme digestions were performed in agarose plugs as described in [Materials and methods](#). As shown in [Fig. 1b](#) and [c](#), telomere length continuously increased up to PD 1000 and no further telomere lengthening was detected in cells between PDs 1000 and 1200 ([Fig. 1c](#), lanes 2–6). The mean TRF lengths were comprised between about 11 kb in cells at PD 167 and more than 100 kb in cells at PDs 1000–1200, with mean lengths around 14, 26, 42, 59 and 80 kb in cells at PDs 241, 334, 407, 505 and 671, respectively.

To determine whether telomere elongation was a property of all, or at least most, cen3tel cells and was not due to the gradual selection of cells with long telomeres, we isolated 4 clones from cen3tel cells at PD 262 and analyzed telomere length in each of them and in parental cells propagated in parallel at successive PDs. Telomere length increased with propagation in parental cells ([Fig. 1d](#), lanes 1–3), as well as in all the 4 clones ([Fig. 1d](#), lanes 4–13).

Taken together, these results indicate that cen3tel cells lost the ability to refrain telomere elongation, which reached values not yet described in human cells.

We then performed fluorescence *in situ* hybridization on metaphase chromosomes from cen3tel cells at different PDs using a fluorescent PNA probe hybridizing with telomeric DNA repeats. Visual analysis revealed that telomeric signal intensities in cells at different PDs displayed the same increasing trend as the mean TRF length (in [Fig. 1e](#) and [f](#), examples of mitoses hybridized with the telomeric

probe from cells at PD 338 and PD 755, respectively, are shown). In addition, hybridization signals were homogeneous among telomeres of the same mitosis. This result, together with the narrow TRF distribution observed in cen3tel cells by gel analysis, indicates that all telomeres are highly elongated during cen3tel cell propagation. Moreover, it suggests that telomere lengthening is not due to ALT activation, which is characterized by a marked heterogeneity in telomere length. The lack of ALT activation was also supported by the absence of ALT PML bodies (data not shown).

3.2. Telomerase activity, telomerase subunit and telomerase regulatory protein expression in cen3tel cells at different PDs

We determined telomerase activity using the TRAP assay in cen3tel cells at different PDs. As shown in [Fig. 2a](#), telomerase activity increased in cells at successive PDs up to around PD 600 (about 6× compared to cen3tel PD 34) and then reached a plateau (quantification of the intensity of the bands is shown in [Fig. S1a](#)). This indicates that telomere lengthening in cen3tel cells is due to an increase in telomerase activity, which parallels cellular transformation. Telomerase activity levels in late PD cen3tel cells were higher than in other tumor cell lines analyzed (e.g. MDA-MB-231, [Fig. 2a](#), lane 14, [Fig. S1a](#)).

Because a typical feature of neoplastically transformed cells is the activation of the *hTERT* gene, we tested whether endogenous *hTERT* had been activated in transformed cen3tel cells, contributing to the

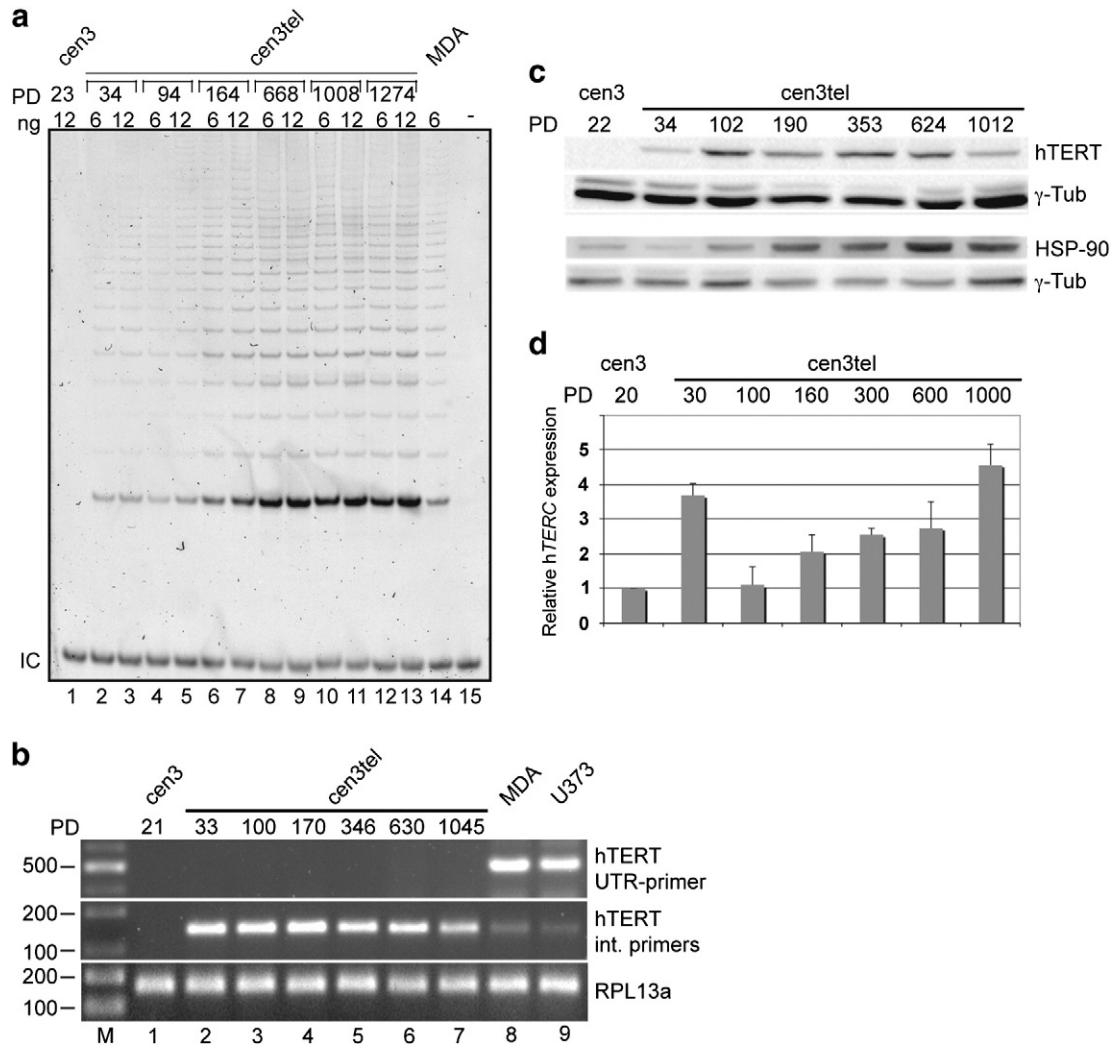


Fig. 2. Telomerase activity and telomerase subunit expression in cen3 primary fibroblasts and cen3tel cells at different propagation stage. (a) Telomerase activity was determined by TRAP assay, the gel was stained using SYBR Gold. IC: internal control; MDA: protein extracts from MDA-MB-231 breast cancer cells used as positive control; above each lane, the amount of protein extract (ng) used is indicated. (b) RT-PCR analysis of endogenous and exogenous hTERT expression. To analyze endogenous hTERT expression, the 3' primer was located in the 3' untranslated region (hTERT UTR-primer) that is not present in the transfected hTERT cDNA. Exogenous hTERT was detected with primer internal to the cDNA. The size (bp) of the molecular weight markers is indicated on the left; RPL13a was used as internal control; MDA-MB-231 (MDA) and U373 cells were used as positive control for endogenous hTERT expression. (c) Western blot analysis of hTERT and Hsp90 expression. γ -Tubulin was used as loading control. (d) Real-time RT-PCR analysis of hTERC expression levels. hTERC expression is indicated relatively to cen3 primary fibroblasts. Error bars represent standard deviations.

increase in telomerase activity. To this regard we performed RT-PCR using a primer within the coding region and another one in the 3' untranslated region, which is not present in the hTERT cDNA used for immortalization. As shown in Fig. 2b (upper panel), no expression of endogenous hTERT could be detected in cen3tel cells at different stages of propagation, even after 40 cycles of PCR. In contrast, RT-PCR performed using primers internal to the hTERT cDNA gave the expected amplification products, the intensity of the amplification bands was similar in all the cen3tel samples and higher than in the tumor cell lines MDA-MB-231 and U373 (Fig. 2b mid panel lanes 2–7 vs. lanes 8, 9).

In the attempt to understand the molecular mechanisms leading to the increase in telomerase activity, we analyzed the expression levels of the hTERT protein and hTERC in cen3tel cells at different PDs, as well as of proteins which regulate telomerase assembly and function, such as Hsp90, its co-chaperon molecule p23, and different isoforms of the protein kinase C (PKC α , β I, β II, δ , ϵ).

Western blot analysis using an antibody against hTERT (Fig. 2c, upper panel), revealed, as expected, the lack of signal in primary

fibroblasts; in cen3tel cells, hTERT expression levels increased (about 6 \times) in cells at PD 102 compared to cells at PD 34, remained roughly constant up to PD 624 and then decreased in cells at PD 1012 (quantification of the band intensity is shown in Fig. S1b).

A similar expression modulation was found for Hsp90. In cells at PD 102, Hsp90 expression increased (about 2 \times compared to parental cen3 fibroblasts, augmented further at PD 190 (about 3 \times) and then remained stable at the subsequent PDs (Fig. 2c, lower panel and Fig. S1c). Thus, both Hsp90 and hTERT levels increased when telomeres started to be elongated, but did not show a continuous increase paralleling the rise in telomere length and telomerase activity. Interestingly, the boost in the expression of both proteins occurred together with the initial phases of transformation.

Western blot analysis did not show changes in the expression of p23 and the different PKC isoforms analyzed during cen3tel cell propagation (data not shown).

hTERC expression in cen3tel cells at different PDs showed an up and down trend (Fig. 2d). In fact, in cen3tel cells around PD 30, it was higher (3.7 \times) than in parental cells, then it went back to values

similar to primary fibroblasts in cells around PD 100 and gradually increased again in cells from PD 160 up to PD 1000 (from about $2 \times$ to $4.6 \times$).

3.3. TRF1 and TRF2 expression and binding to telomeric DNA in cen3tel cells with increasing telomere length

The above results show a continuous increase in telomere length in cen3tel cells from PD 100 up to PD 1000 with the achievement of a length not yet described in human cells. To test whether the telomeric proteins TRF1 and TRF2, key *in cis* regulators of telomere length, played a role in the unrestrained telomere elongation, we analyzed their binding to telomeres in cen3tel cells at subsequent PDs by chromatin immunoprecipitation assays (Fig. 3a–d).

To quantify the proteins bound to the telomeric DNA, chromatin was immunoprecipitated using an anti-TRF1 or anti-TRF2 antibody, after *in vivo* cross-linking between DNA and associated proteins. Cross-linking was then reversed and the DNA co-immunoprecipitated with the proteins was quantified by slot-blot hybridization using a probe for the TTAGGG telomeric repeats (Fig. 3a). In each cell sample, the hybridization signal of the immunoprecipitated telomeric DNA was quantified relatively to the telomeric hybridization signal in the corresponding total DNA, to take into account telomere length, which increased with PDs. The percentage of telomeric DNA immunoprecipitated by TRF1 was around 10% in all the cell samples (10%, 8%, 11% and 10% in cen3tel cells at PDs 168, 333, 652 and 1109, respectively). This result indicates that TRF1 binds all along telomeres ranging in length from about

11 kb (in cells around PD 160) to more than 100 kb (in cells around PD 1000), suggesting that telomere lengthening is not due to a reduced occupancy of TRF1 at telomeres.

A similar conclusion could be drawn for TRF2 binding to telomeres. The efficiency of telomeric chromatin immunoprecipitation with the anti-TRF2 antibody was lower than with the anti-TRF1 antibody (Fig. 3a), but the percentage of telomeric DNA immunoprecipitated was similar in the different samples and was around 1%.

We then analyzed TRF1 and TRF2 total cellular levels in cen3tel cells at different PDs by western blot. Compared to parental fibroblasts and cen3tel cells around PD 30, the expression of both proteins increased in cen3tel cells at the earliest phases of transformation (cen3tel PD 107), showed a further increase in cells around PD 160 and then remained fairly stable (Fig. 3b and Fig. S1d,e). The increased protein levels were not determined by a corresponding increase in the mRNA levels, as demonstrated in quantitative RT-PCR experiments (Fig. 3c). Considering the ratio between TRF1 and TRF2 abundance and telomere length in cells at different PDs (Fig. 3d), it appears that, at the initial phases of transformation (PD 100 and 160), both proteins are in vast excess with respect to telomere length.

3.4. Methylation and expression of subtelomeric loci in cen3tel cells with different telomere length

Since evidence was reported that telomere length could affect methylation levels of subtelomeric DNA [33], we exploited cen3tel cells characterized by highly different telomere lengths to test this

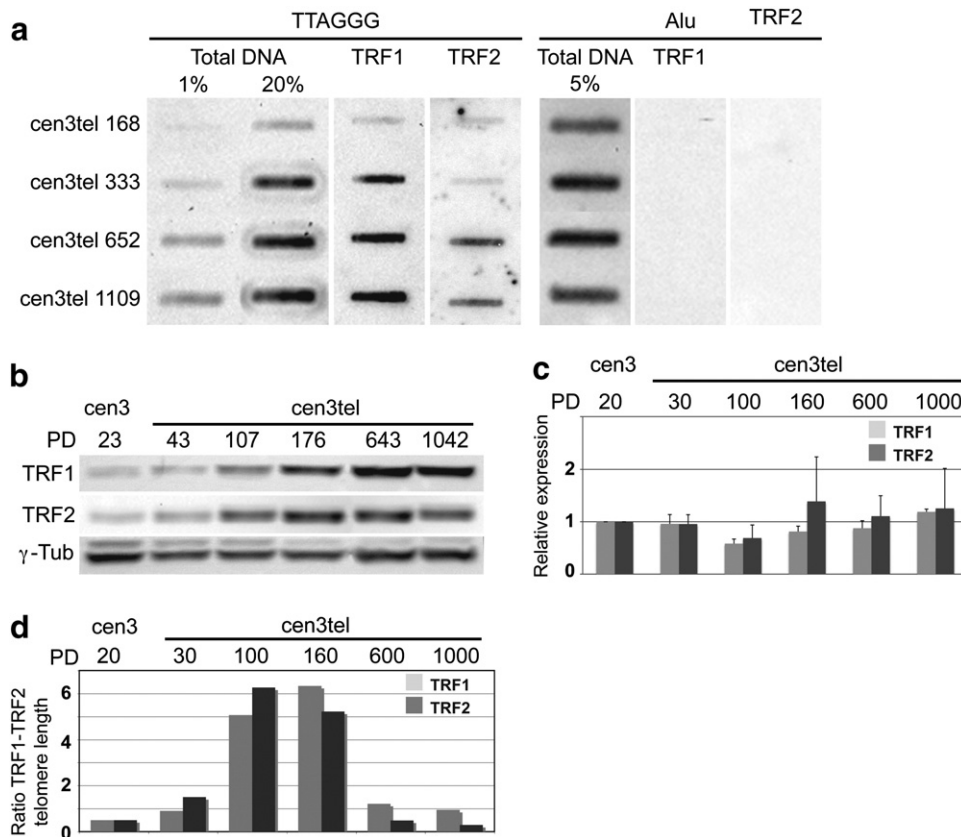


Fig. 3. TRF1 and TRF2 telomere binding and expression. (a) ChIP of telomeric DNA by anti-TRF1 and anti-TRF2 antibodies in cen3tel cells at different stages of propagation. The amount of total DNA blotted, the antibodies used for IP and the hybridization probes (TTAGGG or Alu probes) are indicated at the top. DNA immunoprecipitated by TRF2 was revealed using a ^{32}P -labeled TTAGGG probe, the other membranes were hybridized with a Dig-labeled TTAGGG or ALU probe and the hybridization signal was revealed by chemiluminescence. (b) Western blot analysis of TRF1 and TRF2 expression in cen3 primary and cen3tel cells at different propagation stages. γ -Tubulin was used as loading control. (c) Real time RT-PCR analysis of TRF1 and TRF2 expression in cen3tel cells at different propagation stages. TRF1 and TRF2 expression levels are indicated relatively to cen3 primary fibroblasts. Error bars represent standard deviations. (d) In the plot, for cen3tel cells at different PDs, the ratio between the abundance of TRF1 (gray bars) and TRF2 (black bars) relatively to cen3 primary fibroblasts (as shown in Fig. S1d,e) and the corresponding relative telomere length (calculated by dividing the mean TRF length in each sample by the mean TRF length in primary fibroblasts) is shown.

hypothesis. We used cen3tel cells around PD 100, 300 and 1000 with mean TRF lengths of about 6 kb, 25 kb and greater than 100 kb, respectively. We analyzed the global level of methylation of tandemly repetitive DNA (TRB1 and D4Z4) located at several subtelomeric sites (TRB1: subtelo 2p; D4Z4: subtelo 4q, 10q and 18p) by methyl-DNA immunoprecipitation. DNA samples prepared from cells at the three different stages of propagation were immunoprecipitated with an anti-methyl-cytosine antibody and the amount of DNA immunoprecipitated in the different cell samples was quantified by real-time PCR using primers specific for each repetition family. In Fig. 4a and b, the results of two independent experiments analyzing methylation at the two loci are shown. Although variability was present among the results of the two experiments, we did not find any relationship between telomere length and the degree of methylation at these loci. In particular, in cen3tel cells around PD 1000 we did not detect variations in the subtelomeric region methylation compared to the other cell samples, despite the exceptional telomere length.

We then analyzed whether telomere length could influence the expression of the subtelomeric locus *FRG1*. *FRG1* is located centromeric to the D4Z4 repeats and is involved in Facioscapulohumeral muscular dystrophy [34,35]. In order to analyze *FRG1* expression, a semi-quantitative RT-PCR was performed. Quantification of *FRG1* PCR products, normalized relatively to *GAPDH*, did not reveal differences between the expression of the gene in cen3tel cells around PD 100

and around PD 1000 (Fig. 4c), indicating that very long telomeres do not impair the expression of this subtelomeric locus.

4. Discussion

Telomere maintenance plays a key role in tumorigenesis, where it mainly depends on the activation of hTERT expression, followed by telomerase activity induction. Telomere maintenance and elongation involve several different factors, such as telomerase activity itself, the levels of telomerase components, telomerase ancillary proteins, as well as telomeric proteins. In this work we have investigated telomere dynamics and composition in hTERT immortalized human fibroblasts that underwent neoplastic transformation, showing that transformed cells can lose telomere length homeostasis, reaching telomere length greater than 100 kb, and deregulate the expression of telomere maintenance factors, both in relationship to telomere length and neoplastic transformation.

Analyzing telomere length during the life span of the immortalized fibroblasts, we found that telomeres initially shortened reaching lengths typical of senescent cells, subsequently, started to be elongated attaining a mean length greater than 100 kb. This average length was maintained without detectable variations for at least 200 additional PDs. Telomere lengthening was a property of all or most cells of the population; in fact, in four out of four clones isolated from cells around PD 200, telomeres were elongated during *in vitro* propagation. We did not find evidence of ALT mechanism activation and telomere length was homogenous among chromosome ends within cells and among cells at the same propagation phase.

To our knowledge, the telomere length observed in the cen3tel cellular system represents the upper limit of telomere elongation so far described in human cells. It has been proposed that telomere lengthening beyond a certain threshold, posing constraints to cellular proliferation, could trigger telomere trimming, that is a mechanism for telomere length regulation based on homologous recombination. This mechanism leads to the excision of telomeric DNA and the formation of circles of double-stranded telomeric DNA (t-circles), thus limiting telomere length [36]. Telomere trimming has been described in cells with telomeres shorter than 20 kb. Our results indicate that cells can cope with telomeres much longer than 20 kb without the need of activating mechanisms for telomere shortening. The presence of such super-telomeres did not pose any constraints to cells' survival and proliferation; we did actually find that cell growth increased during propagation of cen3tel cells and was the highest in the cells with the longest telomeres [37]. Moreover, long telomeres were not an obstacle to tumorigenesis, being the cells with the longest telomeres highly aggressive when injected under the skin of immunocompromised mice and able to metastasize when inoculated into the animals' tail vein [24].

Exogenous overexpression of both hTERT and hTERC in human fibroblasts and tumor cell lines was found to lead to higher levels of telomerase activity and greater telomere lengthening than the ectopic expression of hTERT alone [22], indicating that both telomerase subunits regulate and are limiting for telomerase activity. In our cellular system, we found that telomere lengthening was linked to a progressive increase in telomerase activity, which reached levels higher than in tumor cell lines expressing endogenous TERT. Both hTERT and hTERC expression levels rose during cen3tel cell life span, although with different trends. As expected, hTERT was undetectable in primary fibroblasts and expressed in transduced cells around PD 30, then its levels increased in cells at the early phases of transformation without further increase thereafter. Neoplastic transformation was not associated with reactivation of endogenous hTERT or transcriptional regulation of the exogenous hTERT cDNA, indicating that high hTERT levels can also be achieved through post-transcriptional regulation mechanisms.

hTERC was expressed in primary fibroblasts, its levels increased as soon as hTERT was expressed in the cells, and decreased thereafter, in

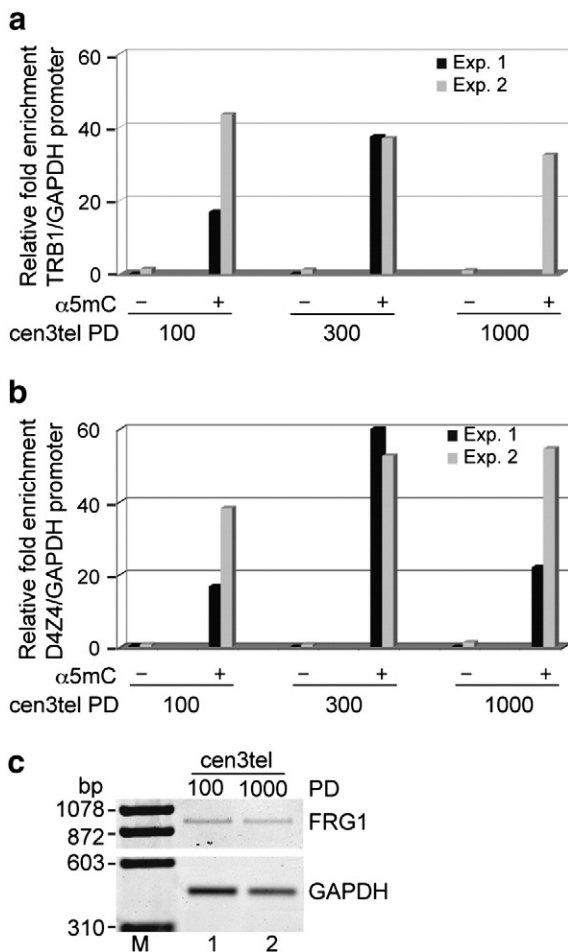


Fig. 4. Methylation and gene expression in subtelomeric regions of cen3tel cells with different telomere length. For methylation analysis (a, b) DNA was extracted from cen3tel cells at different PDs and immunoprecipitated with anti methyl-cytosine antibodies; the amount of TRB1 (a) and D4Z4 (b) sequences precipitated in the different cell lines was quantified by real-time PCR and normalized relatively to *GAPDH* promoter sequences. (c) RT-PCR analysis of *FRG1* expression in cen3tel cells at PD 108 and 1008. The size (bp) of the molecular weight markers is indicated on the left.

parallel to telomere shortening, then gradually increased during cell propagation, reaching the highest levels in cells around PD 1000. Considering the expression of each telomerase subunit and telomerase activity in cells at different stages of propagation, we can infer that the reciprocal levels of both telomerase subunits are important to determine telomerase activity. In fact, in cen3tel cells around PD 100, the high hTERT expression relatively to cells at the preceding stage did not lead to an increase in telomerase activity, probably because of the low hTERC expression. On the other hand, in cen3tel cells around PD 1000, despite the lower hTERT levels compared to cells at the previous phase, telomerase activity was not compromised, probably because of the higher hTERC expression. These results confirm a role of hTERC in limiting or enhancing telomerase activity and determining telomere length, as previously shown in cellular systems in which hTERC had been exogenously overexpressed [22,23]. Moreover, they indicate that hTERC expression can spontaneously undergo deregulation during neoplastic transformation, contributing to the induction of a highly efficient enzyme.

Evidence has been reported that auxiliary telomerase proteins, such as different protein kinase C isoforms and the chaperon proteins p23 and Hsp90, are involved in telomerase activity regulation [38,39] and are overexpressed in several tumors, thus we analyzed the expression of these proteins in cen3tel cells at different stages of propagation. We found that PKC isoform and p23 expression levels were stable during cell propagation, suggesting that these proteins do not play a role in determining the increase in telomerase activity and telomere length observed in cen3tel cells. In contrast, we did find a modulation of Hsp90 expression, with increased protein levels in transformed and tumorigenic cells compared to parental fibroblasts and early passage cen3tel cells, which could contribute to determine the high telomerase activity observed in these cells. On the other hand, the high Hsp90 expression in transformed and tumorigenic cen3tel cells could also play a role in determining their transformed phenotype; in fact, Hsp90 is known to be overexpressed in cancer cells, in which contribute to tumorigenesis protecting different mutated and overexpressed oncoproteins from misfolding and degradation [40].

TRF1 and TRF2 are well known negative regulators of telomere length in mammalian cells, being part of a negative feedback loop that prevents telomere elongation *in cis* [5–7]: the high number of bound telomeric proteins on long telomeres would constrain their lengthening. In cen3tel cells, ChIP experiments showed that the amount of TRF1 and TRF2 bound to telomeres increased with telomere length, indicating that telomeres can be maintained in an extendible state over a range of lengths between 10 and 100 kb, despite TRF1 and TRF2 binding throughout all their length. Although TRF1 and TRF2 binding to telomeres does not seem to be involved in telomere length deregulation in cen3tel cells, we cannot exclude that variations in the expression or binding of proteins interacting with the telomeric 3' overhang, such as POT1 and TPP1, could contribute to this phenomenon [4].

As well as hTERT and Hsp90, TRF1 and TRF2 cellular levels increased concomitantly with transformation, probably because of post-transcriptional regulation mechanisms, since no variations in the corresponding mRNAs were observed in cells at different PDs. The vast excess of TRF1 and TRF2 with respect to telomere length in cells at the initial phases of transformation suggests that these proteins can play a role in the transformation process itself. This is in agreement with the hypothesis that these proteins play also a role in tumorigenesis. To this regard, evidence has been reported that TRF1 and TRF2 expression is increased in different types of human cancers, such as gastric, hepatocellular and lung carcinomas, as well as in human breast-tumor derived cell lines [41–44]. Moreover, a role for TRF2 in tumorigenesis was confirmed by showing increased carcinogenesis in TRF2 overexpressing mice [45], on the one hand, and reduced tumorigenicity of malignant cell lines after TRF2

inhibition [46], on the other hand. The mechanism by which TRF1 and TRF2 are linked to tumorigenesis is still unknown. Analysis of TRF2-overexpressing telomerase-deficient mice suggested a role for TRF2 in telomere shortening and chromosomally instability-driven carcinogenesis [47]. However, our results indicate that this cannot be the only mechanism, given the very long and stable telomeres characterizing cen3tel cells. The recent observation that TRF1 and TRF2 also bind to intrachromosomal sequences often located close to genes or within introns [48] opens up the possibility that these telomeric proteins participate in carcinogenesis regulating the expression of genes relevant to this process.

Besides telomeric proteins and telomerase activity, epigenetic modifications of telomeric and subtelomeric chromatin have been implicated in telomere maintenance [49]. It has been proposed that the loss of heterochromatic marks in telomeric and subtelomeric regions leads to telomere elongation. Subtelomeric DNA demethylation due to the loss of the expression of the maintenance DNA methyl-transferase 1 in mouse ES cells has been shown to lead to telomere lengthening, while telomere shortening in telomerase deficient mouse models has been found to be associated with subtelomeric DNA demethylation, suggesting that subtelomeric DNA epigenetic status and telomere length can reciprocally modulate each other. Contrasting results have been presented concerning the possible relationship between subtelomeric DNA methylation and telomere length in cancer cells [50,51]. Moreover, in a recent paper, Gadalla et al. [52], studying DNA methylation at the D4Z4 subtelomeric repeat in lymphocytes from a cohort of Dyskeratosis congenita patients and their mutation negative relatives, found a positive correlation between methylation levels and telomere length in the patients and a negative, but no significant correlation, in the normal individuals. In our cellular system, we analyzed global DNA methylation of the tandemly repeated TRB1 sequence, located at the 2p subtelomere, and D4Z4 DNA, located at the 4q, 10q and 18p subtelomeres, in cen3tel cells at three different stages of propagation with mean TRF length around 6, 25 and more than 100 kb, respectively, and we did not find a relationship between telomere length and global DNA methylation levels. We cannot exclude that telomere length influences DNA methylation at specific subtelomeric sites; however, our data indicate that massive telomere elongation in human transformed fibroblasts is not associated with a massive change in DNA methylation at subtelomeres and, *vice versa*, a massive decrease in DNA methylation at subtelomeres is not required for telomere elongation. In agreement with this observation, we did not observe variations in the expression of the *FRG1* gene, located at 4q [34], in cells around PD 100 and in cells around PD 1000, which have telomeres shorter than 10 kb and longer than 100 kb, respectively.

5. Conclusions

In conclusion, in this work we have shown that transformed human fibroblasts can reach a telomere length greater than 100 kb without any impairment in cellular growth and tumorigenic potential. The genesis of super-telomeres is associated with an increase in hTERT and hTERC expression during transformation, which leads to high levels of telomerase activity. Moreover, our data indicate that the relative levels of the two telomerase subunits are crucial for the determination of the enzymatic activity. Although we cannot define a causal relationship between cellular transformation and the loss of telomere length homeostasis, our results show that the initial phases of transformation coincides with the increase in the expression of proteins involved in telomere metabolism, such as TRF1, TRF2, Hsp90 and hTERT itself, suggesting a dual role for these proteins in tumorigenesis and telomere maintenance.

Supplementary data to this article can be found online at <http://dx.doi.org/10.1016/j.bbamcr.2013.03.030>.

Acknowledgements

We are grateful to Dr. Davide Gabellini (San Raffaele Scientific Institute, Milan, Italy) for FRG1 primers and suggestions for the analysis of its expression. Work in C.M. laboratory is supported by Fondazione Cariplo (grant n. 2011-0370).

References

- [1] E.H. Blackburn, C.W. Greider, J.W. Szostak, Telomeres and telomerase: the path from maize, Tetrahymena and yeast to human cancer and aging, *Nat. Med.* 12 (2006) 1133–1138.
- [2] V.L. Makarov, Y. Hirose, J.P. Langmore, Long G tails at both ends of human chromosomes suggest a C strand degradation mechanism for telomere shortening, *Cell* 88 (1997) 657–666.
- [3] E. Gilson, V. Geli, How telomeres are replicated, *Nat. Rev. Mol. Cell Biol.* 8 (2007) 825–838.
- [4] W. Palm, T. de Lange, How shelterin protects mammalian telomeres, *Annu. Rev. Genet.* 42 (2008) 301–334.
- [5] B. van Steensel, T. de Lange, Control of telomere length by the human telomeric protein TRF1, *Nature* 385 (1997) 740–743.
- [6] K. Ancelin, M. Brunori, S. Bauwens, C.E. Koering, C. Brun, M. Ricoul, J.P. Pommier, L. Sabatier, E. Gilson, Targeting assay to study the cis functions of human telomeric proteins: evidence for inhibition of telomerase by TRF1 and for activation of telomere degradation by TRF2, *Mol. Cell. Biol.* 22 (2002) 3474–3487.
- [7] K.K. Takai, S. Hooper, S. Blackwood, R. Gandhi, T. de Lange, In vivo stoichiometry of shelterin components, *J. Biol. Chem.* 285 (2010) 1457–1467.
- [8] D. Loayza, T. De Lange, POT1 as a terminal transducer of TRF1 telomere length control, *Nature* 423 (2003) 1013–1018.
- [9] E.H. Blackburn, K. Collins, Telomerase: an RNP enzyme synthesizes DNA, *Cold Spring Harb. Perspect. Biol.* 3 (2011).
- [10] S.B. Cohen, M.E. Graham, G.O. Lovrecz, N. Bache, P.J. Robinson, R.R. Reddel, Protein composition of catalytically active human telomerase from immortal cells, *Science* 315 (2007) 1850–1853.
- [11] K. Masutomi, E.Y. Yu, S. Khurts, I. Ben-Porath, J.L. Currier, G.B. Metz, M.W. Brooks, S. Kaneko, S. Murakami, J.A. DeCaprio, R.A. Weinberg, S.A. Stewart, W.C. Hahn, Telomerase maintains telomere structure in normal human cells, *Cell* 114 (2003) 241–253.
- [12] F. Rodier, J. Campisi, Four faces of cellular senescence, *J. Cell Biol.* 192 (2011) 547–556.
- [13] F. d'Adda di Fagagna, P.M. Reaper, L. Clay-Farrace, H. Fiegler, P. Carr, T. Von Zglinicki, G. Saretzki, N.P. Carter, S.P. Jackson, A DNA damage checkpoint response in telomere-initiated senescence, *Nature* 426 (2003) 194–198, (Epub 2003 Nov 2005).
- [14] C.B. Harley, Telomere loss: mitotic clock or genetic time bomb? *Mutat. Res.* 256 (1991) 271–282.
- [15] J.W. Shay, S. Bacchetti, A survey of telomerase activity in human cancer, *Eur. J. Cancer* 33 (1997) 787–791.
- [16] T.M. Bryan, A. Englezou, L. Dalla-Pozza, M.A. Dunham, R.R. Reddel, Evidence for an alternative mechanism for maintaining telomere length in human tumors and tumor-derived cell lines, *Nat. Med.* 3 (1997) 1271–1274.
- [17] A.J. Cesare, R.R. Reddel, Alternative lengthening of telomeres: models, mechanisms and implications, *Nat. Rev. Genet.* 11 (2010) 319–330.
- [18] C. Belgiovine, I. Chiodi, C. Mondello, Telomerase: cellular immortalization and neoplastic transformation. Multiple functions of a multifaceted complex, *Cytogenet. Genome Res.* 122 (2008) 255–262.
- [19] A.G. Bodnar, M. Ouellette, M. Frolkis, S.E. Holt, C.P. Chiu, G.B. Morin, C.B. Harley, J.W. Shay, S. Lichtsteiner, W.E. Wright, Extension of life-span by introduction of telomerase into normal human cells, *Science* 279 (1998) 349–352.
- [20] M.M. Ouellette, D.L. Aisner, I. Savre-Train, W.E. Wright, J.W. Shay, Telomerase activity does not always imply telomere maintenance, *Biochem. Biophys. Res. Commun.* 254 (1999) 795–803.
- [21] S. Zongaro, A. Verri, E. Giulotto, C. Mondello, Telomere length and radiosensitivity in human fibroblast clones immortalized by ectopic telomerase expression, *Oncol. Rep.* 19 (2008) 1605–1609.
- [22] G. Cristofari, J. Lingner, Telomere length homeostasis requires that telomerase levels are limiting, *EMBO J.* 25 (2006) 565–574.
- [23] P. Vidale, E. Magnani, S.G. Nergadze, M. Santagostino, G. Cristofari, A. Smirnova, C. Mondello, E. Giulotto, The catalytic and the RNA subunits of human telomerase are required to immortalize equid primary fibroblasts, *Chromosoma* 121 (2012) 475–488.
- [24] C. Belgiovine, R. Frapolli, K. Bonezzi, I. Chiodi, F. Favero, M. Mello-Grand, A.P. Dei Tos, E. Giulotto, G. Tarabozzi, M. D'Incalci, C. Mondello, Reduced expression of the ROCK inhibitor Rnd3 is associated with increased invasiveness and metastatic potential in mesenchymal tumor cells, *PLoS One* 5 (2010) e14154.
- [25] C. Mondello, M. Chiesa, P. Rebuzzini, S. Zongaro, A. Verri, T. Colombo, E. Giulotto, M. D'Incalci, C. Franceschi, F. Nuzzo, Karyotype instability and anchorage-independent growth in telomerase-immortalized fibroblasts from two centenarian individuals, *Biochem. Biophys. Res. Commun.* 308 (2003) 914–921.
- [26] P. Ostano, S. Bione, C. Belgiovine, I. Chiodi, C. Ghimenti, A.I. Scovassi, G. Chiorino, C. Mondello, Cross-analysis of gene and miRNA genome-wide expression profiles in human fibroblasts at different stages of transformation, *OMICS* 16 (2012) 24–36.
- [27] S. Zongaro, E. de Stanchina, T. Colombo, M. D'Incalci, E. Giulotto, C. Mondello, Stepwise neoplastic transformation of a telomerase immortalized fibroblast cell line, *Cancer Res.* 65 (2005) 11411–11418.
- [28] C.B. Harley, A.B. Futcher, C.W. Greider, Telomeres shorten during ageing of human fibroblasts, *Nature* 345 (1990) 458–460.
- [29] P.M. Lansdorp, N.P. Verwoerd, F.M. van de Rijke, V. Dragowska, M.T. Little, R.W. Dirks, A.K. Raap, H.J. Tanke, Heterogeneity in telomere length of human chromosomes, *Hum. Mol. Genet.* 5 (1996) 685–691.
- [30] X. Yi, V.M. Tesmer, I. Savre-Train, J.W. Shay, W.E. Wright, Both transcriptional and posttranscriptional mechanisms regulate human telomerase template RNA levels, *Mol. Cell. Biol.* 19 (1999) 3989–3997.
- [31] E. Gilson, B. Horard, Comprehensive DNA methylation profiling of human repetitive DNA elements using an MeDIP-on-RepArray assay, *Methods Mol. Biol.* 859 (2012) 267–291.
- [32] B. Horard, A. Eymery, G. Fourel, N. Vassetzky, J. Puechberty, G. Roizes, K. Lebrigand, P. Barbry, A. Laugraud, C. Gautier, E.B. Simon, F. Devaux, F. Magdinier, C. Vourc'h, E. Gilson, Global analysis of DNA methylation and transcription of human repetitive sequences, *Epigenetics* 4 (2009) 339–350.
- [33] R. Benetti, M. Garcia-Cao, M.A. Blasco, Telomere length regulates the epigenetic status of mammalian telomeres and subtelomeres, *Nat. Genet.* 39 (2007) 243–250.
- [34] J.C. van Deutekom, C. Wijmenga, E.A. van Tienhoven, A.M. Gruter, J.E. Hewitt, G.W. Padberg, G.J. van Ommen, M.H. Hofker, R.R. Frants, FSHD associated DNA rearrangements are due to deletions of integral copies of a 3.2 kb tandemly repeated unit, *Hum. Mol. Genet.* 2 (1993) 2037–2042.
- [35] D. Gabellini, G. D'Antona, M. Moggio, A. Prella, C. Zecca, R. Adami, B. Angeletti, P. Ciscato, M.A. Pellegrino, R. Bottinelli, M.R. Green, R. Tupler, Facioscapulohumeral muscular dystrophy in mice overexpressing FRG1, *Nature* 439 (2006) 973–977.
- [36] H.A. Pickett, A.J. Cesare, R.L. Johnston, A.A. Neumann, R.R. Reddel, Control of telomere length by a trimming mechanism that involves generation of t-circles, *EMBO J.* 28 (2009) 799–809.
- [37] F. Donà, I. Chiodi, C. Belgiovine, T. Raineri, R. Ricotti, C. Mondello, A.I. Scovassi, Poly(ADP-ribosylation) and neoplastic transformation: effect of PARP inhibitors, *Curr. Pharm. Biotechnol.* (Mar. 20 2012), (Epub ahead of print).
- [38] J.T. Chang, Y.C. Lu, Y.J. Chen, C.P. Tseng, Y.L. Chen, C.W. Fang, A.J. Cheng, hTERT phosphorylation by PKC is essential for telomerase holoprotein integrity and enzyme activity in head neck cancer cells, *Bur. J. Cancer* 94 (2006) 870–878.
- [39] D.C. DeZwaan, B.C. Freeman, HSP90 manages the ends, *Trends Biochem. Sci.* 35 (2010) 384–391.
- [40] J. Trepel, M. Mollapour, G. Giaccone, L. Neckers, Targeting the dynamic HSP90 complex in cancer, *Nat. Rev. Cancer* 10 (2010) 537–549.
- [41] N. Matsutani, H. Yokozaki, E. Tahara, H. Tahara, H. Kuniyasu, K. Haruma, K. Chayama, W. Yasui, E. Tahara, Expression of telomeric repeat binding factor 1 and 2 and TRF1-interacting nuclear protein 2 in human gastric carcinomas, *Int. J. Oncol.* 19 (2001) 507–512.
- [42] B.K. Oh, Y.J. Kim, C. Park, Y.N. Park, Up-regulation of telomere-binding proteins, TRF1, TRF2, and TIN2 is related to telomere shortening during human multistep hepatocarcinogenesis, *Am. J. Pathol.* 166 (2005) 73–80.
- [43] T. Nijjar, E. Bassett, J. Garbe, Y. Takenaka, M.R. Stampfer, D. Gilley, P. Yaswen, Accumulation and altered localization of telomere-associated protein TRF2 in immortally transformed and tumor-derived human breast cells, *Oncogene* 24 (2005) 3369–3376.
- [44] K. Nakanishi, T. Kawai, F. Kumaki, S. Hiroi, M. Mukai, E. Ikeda, C.E. Koering, E. Gilson, Expression of mRNAs for telomeric repeat binding factor (TRF)-1 and TRF2 in atypical adenomatous hyperplasia and adenocarcinoma of the lung, *Clin. Cancer Res.* 9 (2003) 1105–1111.
- [45] P. Munoz, R. Blanco, M.A. Blasco, Role of the TRF2 telomeric protein in cancer and ageing, *Cell Cycle* 5 (2006) 718–721.
- [46] A. Biroccio, A. Rizzo, R. Elli, C.E. Koering, A. Belleville, B. Benassi, C. Leonetti, M.F. Stevens, M. D'Incalci, G. Zupi, E. Gilson, TRF2 inhibition triggers apoptosis and reduces tumorigenicity of human melanoma cells, *Bur. J. Cancer* 94 (2006) 1881–1888.
- [47] R. Blanco, P. Munoz, J.M. Flores, P. Klatt, M.A. Blasco, Telomerase abrogation dramatically accelerates TRF2-induced epithelial carcinogenesis, *Genes Dev.* 21 (2007) 206–220.
- [48] T. Simonet, L.E. Zaragosi, C. Philippe, K. Lebrigand, C. Schouteden, A. Augereau, S. Bauwens, J. Ye, M. Santagostino, E. Giulotto, F. Magdinier, B. Horard, P. Barbry, R. Waldmann, E. Gilson, The human TTAGGG repeat factors 1 and 2 bind to a subset of interstitial telomeric sequences and satellite repeats, *Cell Res.* 21 (2011) 1028–1038.
- [49] M.A. Blasco, The epigenetic regulation of mammalian telomeres, *Nat. Rev. Genet.* 8 (2007) 299–309.
- [50] B.K. Oh, T.H. Um, G.H. Choi, Y.N. Park, Frequent changes in subtelomeric DNA methylation patterns and its relevance to telomere regulation during human hepatocarcinogenesis, *Int. J. Cancer* 128 (2011) 857–868.
- [51] E. Vera, A. Canela, M.F. Fraga, M. Esteller, M.A. Blasco, Epigenetic regulation of telomeres in human cancer, *Oncogene* 27 (2008) 6817–6833.
- [52] S.M. Gadalla, H.A. Katki, F.M. Shebl, N. Giri, B.P. Alter, S.A. Savage, The relationship between DNA methylation and telomere length in dyskeratosis congenita, *Aging Cell* 11 (2012) 24–28.